Synthesis, spectroscopic and computational characterization of the tautomerism of pyrazoline derivatives from chalcones

Fábio Balbino Miguel, Juliana Arantes Dantas, Stefany Amorim, Gustavo F.S. Andrade, Luiz Antônio Sodré Costa, Mara Rubia Costa Couri

PII: S1386-1425(15)30090-1
DOI: http://dx.doi.org/10.1016/j.saa.2015.07.041
Reference: SAA 13940

To appear in: *Spectrochimica Acta Part A: Molecular and Biomolecular Spectroscopy*

Received Date: 12 March 2015
Revised Date: 3 June 2015
Accepted Date: 7 July 2015

Please cite this article as: F.B. Miguel, J.A. Dantas, S. Amorim, G.F.S. Andrade, L.A.S. Costa, M.R.C. Couri, Synthesis, spectroscopic and computational characterization of the tautomerism of pyrazoline derivatives from chalcones, *Spectrochimica Acta Part A: Molecular and Biomolecular Spectroscopy* (2015), doi: http://dx.doi.org/10.1016/j.saa.2015.07.041

Synthesis, spectroscopic and computational characterization of the tautomerism of pyrazoline derivatives from chalcones

Fábio Balbino Miguel[a], Juliana Arantes Dantas[a], Stefany Amorim[b], Gustavo F. S. Andrade[b], Luiz Antônio Sodré Costa[c], Mara Rubia Costa Couri[a,*]

[a]NUPEQ – Núcleo Multifuncional de Pesquisas Químicas, Departamento de Química, Instituto de Ciências Exatas, Universidade Federal de Juiz de Fora, 36036-900, Juiz de Fora-MG, Brazil.

[b]NEEM – Laboratório de Nanoestruturas Plasmônicas, Núcleo de Espectroscopia e Estrutura Molecular, Departamento de Química, Instituto de Ciências Exatas, Universidade Federal de Juiz de Fora, 36036-900, Juiz de Fora- MG, Brazil.

[c]NEQC – Núcleo de Estudos em Química Computacional, Departamento de Química, Instituto de Ciências Exatas, Universidade Federal de Juiz de Fora, 36036-900, Juiz de Fora-MG, Brazil.

*Corresponding author: mara.rubia@ufjf.edu.br

ABSTRACT: In the present study a series of novel pyrazolines derivatives has been synthesized, and their structures assigned on the basis of FT-Raman, ^{1}H and ^{13}C NMR spectral data and computational DFT calculations. A joint computational study using B3LYP/6-311G(2d,2p) density functional theory and FT-Raman investigation on the tautomerism of 3-(4-substituted-phenyl)-4,5-dihydro-5-(4-substituted-phenyl)pyrazole-1-carbothioamide and 3-(4-substituted-phenyl)-4,5-dihydro-5-(4-substituted-phenyl)pyrazole-1-carboxamide are presented. The structures were characterized as a minimum in the potential energy surface using DFT. The calculated Raman and NMR spectra were of such remarkable agreement to the experimental results that the equilibrium between tautomeric forms has been discussed in detail. Our study suggests the existence of tautomers, the carboxamide/carbothioamide group may tautomerize, in the solid state or in solution. Thermodynamic data calculated suggests that the $R(C=S)NH_2$ and $R(C=O)NH_2$ species are more stable than the R(C=NH)SH and R(C=NH)OH species. Additionally, results found for the ^{1}H-NMR shifting, pointed out to which structure is present.

KEYWORDS: Synthesis, Tautomerism, Chalcones, Pyrazolines, Raman, DFT

1. INTRODUCTION

The interest in obtaining chalcones and their pyrazolines analogues has grown in the past ten years because of numerous pharmacological properties have been discovered, namely: antimicrobial [1-6], anti-tubercular [1,7,8], anticancer [8,9], anti-inflammatory [8] and antioxidant [5] activities. The wide range of pharmacological activities of these compounds shows the importance of this family of heterocyclic compounds in the area of medicinal chemistry. Consequently, the use of known methods for the synthesis and characterization of this class of compounds constitutes an important field of synthetic organic chemistry [2,10,11].

In general, 2-pyrazolines derivatives are obtained by condensation between α,β-unsaturated carbonyl compound and hydrazine derivatives [10,12,13]. In the case of compounds having a large number of unsaturations, an effect known as tautomerism may occur. The study of the tautomerism may contribute to the understanding of the structural/biological activity of this family of compounds [14,15]. Among the available spectroscopic tools, Raman spectroscopy has been suggested as a powerful technique to identify tautomers. The possibility of understanding the substances fingerprints in a Raman spectrum, which may be assigned to characteristics frequencies for each tautomeric form, has led to the development of this spectroscopic technique as an important tool for the characterization of tautomeric forms [16-19].

On the other hand, nuclear magnetic resonance (NMR) spectroscopy was introduced into organic chemistry to determine carbon skeleton of the organic compounds, plays an enormously important role in studying various chemical interactions, tautomeric rearrangement, purity and authenticity of molecules. In this context, NMR is a widely used and very powerful tool for the characterization of tautomeric equilibrium for some important compounds such as histidine and D-fructose, among others [20,21]. The use of NMR techniques for the description of tautomeric equilibrium relies on chemical systems that present slow enough proton exchange for both systems to be measured in solution [22,23]. Additionally, the support from quantum chemistry predictions is usually essential for the interpretation of NMR results [22,24]. Molecular structure, conformational stability and vibrational frequencies have been studied by ab initio and DFT methods [22,25-28]. The support of quantum chemistry methods, mostly based on density functional theory (DFT), has been essential for the interpretation of both NMR and Raman spectroscopy results for the

assignment of spectra from both techniques, as well as on the calculation of total energy changes between different tautomeric species. Recently, Hadda's research group has published a benchmark paper featuring the tautomerism of some curcumin derivatives which have several biological significance [29].

In this report, a series of pyrazolines derivatives was synthesized and the structures assigned on the basis of FT-Raman, ^{1}H and ^{13}C NMR spectral data and computational DFT calculations. Furthermore, theoretical calculations were also used to check on the stability of such compounds. Here, the spectroscopic techniques have been used along with computational calculation for the evaluation of the tautomerism. Based on the spectroscopic data experimentally obtained, full quantum mechanical calculations have been applied to pyrazoline derivatives (Figure 1).

2. MATERIAL AND METHODS

All procedures for the synthesis of pyrazoline derivatives **18-47** are presented in Supporting Information as well as the structural data collected. NMR spectra and other details about some procedures related to computational details are also presented.

2.1. Synthesis

In order to synthesize *O*-alkylated chalcone derivatives **1-17**, 4-hydroxybenzaldehyde was initially alkylated (79–99% yield), using a Williamson ether synthesis [38-40], with K_2CO_3 and butyl, hexyl, octyl, nonyl, decyl, dodecyl or tetradecyl bromide in DMF. Commercial aldehydes 4-bromobenzaldehyde, 4-methoxybenzaldehyde, 4-(dimethylamino)benzaldehyde, 4-methylbenzaldehyde, 4-chlorobenzaldehyde, benzaldehyde and *O*-alkylated aldehydes were then treated with equimolar quantities of the acetophenone or 1-(4-fluorophenyl)ethanone and NaOH (1.5 eq.) in ethanol (Scheme 1), using Claisen–Schmidt reaction [40-43]. All the compounds were purified by recrystallization using a suitable solvent and the assignment of the structures is fully supported by their characteristic chemical shift values.

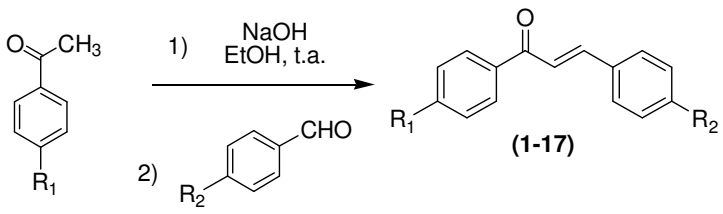

1: R_1 = H; R_2 = $O(CH_2)_3CH_3$ (79%)
2: R_1 = H; R_2 = $O(CH_2)_5CH_3$ (99%)
3: R_1 = H; R_2 = $O(CH_2)_7CH_3$ (95%)
4: R_1 = H; R_2 = $O(CH_2)_8CH_3$ (52%)
5: R_1 = H; R_2 = $O(CH_2)_9CH_3$ (95%)
6: R_1 = H; R_2 = $O(CH_2)_{11}CH_3$ (96%)
7: R_1 = H; R_2 = $O(CH_2)_{13}CH_3$ (99%)
8: R_1 = F; R_2 = $O(CH_2)_7CH_3$ (66%)
9: R_1 = F; R_2 = $O(CH_2)_8CH_3$ (72%)
10: R_1 = F; R_2 = $O(CH_2)_9CH_3$ (51%)
11: R_1 = F; R_2 = $O(CH_2)_{13}CH_3$ (74%)
12: R_1 = F; R_2 = Br (42%)
13: R_1 = F; R_2 = OMe (38%)
14: R_1 = F; R_2 = NMe_2 (28%)
15: R_1 = F; R_2 = Me (55%)
16: R_1 = F; R_2 = Cl (69%)
17: R_1 = F; R_2 = H (72%)

Scheme 1. General synthesis of chalcone derivatives.

The pyrazolines **18-47** were prepared by treatment of chalcone derivatives in ethanol, hydrazine derivatives under basic conditions (Scheme 2). All the compounds were purified by recrystallization using a suitable solvent. After purification procedures, pyrazolines **18-47** were characterized by ^{1}H NMR, ^{13}C NMR spectral data.

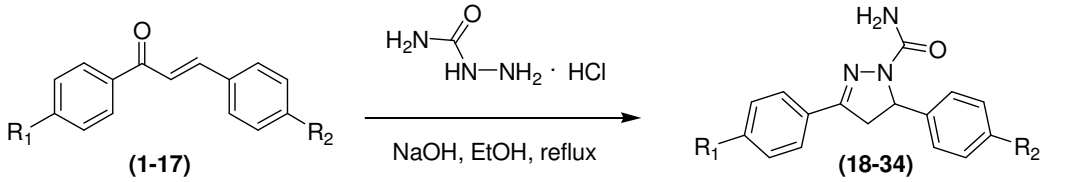

1: R_1 = H; R_2 = $O(CH_2)_3CH_3$
2: R_1 = H; R_2 = $O(CH_2)_5CH_3$
3: R_1 = H; R_2 = $O(CH_2)_7CH_3$
4: R_1 = H; R_2 = $O(CH_2)_8CH_3$
5: R_1 = H; R_2 = $O(CH_2)_9CH_3$
6: R_1 = H; R_2 = $O(CH_2)_{11}CH_3$
7: R_1 = H; R_2 = $O(CH_2)_{13}CH_3$
8: R_1 = F; R_2 = $O(CH_2)_7CH_3$
9: R_1 = F; R_2 = $O(CH_2)_8CH_3$
10: R_1 = F; R_2 = $O(CH_2)_9CH_3$
11: R_1 = H; R_2 = $O(CH_2)_{13}CH_3$
12: R_1 = F; R_2 = Br
13: R_1 = F; R_2 = OMe
14: R_1 = F; R_2 = NMe_2
15: R_1 = F; R_2 = Me
16: R_1 = F; R_2 = Cl
17: R_1 = F; R_2 = H

18: R_1 = H; R_2 = $O(CH_2)_3CH_3$ (30%)
19: R_1 = H; R_2 = $O(CH_2)_5CH_3$ (11%)
20: R_1 = H; R_2 = $O(CH_2)_7CH_3$ (34%)
21: R_1 = H; R_2 = $O(CH_2)_8CH_3$ (25%)
22: R_1 = H; R_2 = $O(CH_2)_9CH_3$ (16%)
23: R_1 = H; R_2 = $O(CH_2)_{11}CH_3$ (22%)
24: R_1 = H; R_2 = $O(CH_2)_{13}CH_3$ (15%)
25: R_1 = F; R_2 = $O(CH_2)_7CH_3$ (23%)
26: R_1 = F; R_2 = $O(CH_2)_8CH_3$ (24%)
27: R_1 = F; R_2 = $O(CH_2)_9CH_3$ (22%)
28: R_1 = F; R_2 = $O(CH_2)_{13}CH_3$ (25%)
29: R_1 = F; R_2 = Br (9%)
30: R_1 = F; R_2 = OMe (15%)
31: R_1 = F; R_2 = NMe_2 (17%)
32: R_1 = F; R_2 = Me (13%)
33: R_1 = F; R_2 = Cl (15%)
34: R_1 = F; R_2 = H (10%)

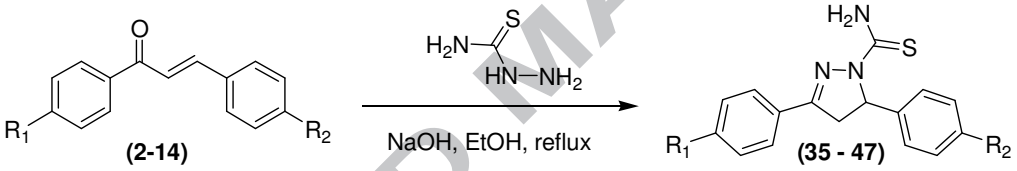

2: R_1 = H; R_2 = $O(CH_2)_5CH_3$
3: R_1 = H; R_2 = $O(CH_2)_7CH_3$
4: R_1 = H; R_2 = $O(CH_2)_8CH_3$
5: R_1 = H; R_2 = $O(CH_2)_9CH_3$
6: R_1 = H; R_2 = $O(CH_2)_{11}CH_3$
7: R_1 = H; R_2 = $O(CH_2)_{13}CH_3$
8: R_1 = F; R_2 = $O(CH_2)_7CH_3$
9: R_1 = F; R_2 = $O(CH_2)_8CH_3$
10: R_1 = F; R_2 = $O(CH_2)_9CH_3$
11: R_1 = H; R_2 = $O(CH_2)_{13}CH_3$
12: R_1 = F; R_2 = Br
13: R_1 = F; R_2 = OMe
14: R_1 = F; R_2 = NMe_2

35: R_1 = H; R_2 = $O(CH_2)_5CH_3$ (29%)
36: R_1 = H; R_2 = $O(CH_2)_7CH_3$ (27%)
37: R_1 = H; R_2 = $O(CH_2)_8CH_3$ (14%)
38: R_1 = H; R_2 = $O(CH_2)_9CH_3$ (29%)
39: R_1 = H; R_2 = $O(CH_2)_{11}CH_3$ (22%)
40: R_1 = H; R_2 = $O(CH_2)_{13}CH_3$ (37%)
41: R_1 = F; R_2 = $O(CH_2)_7CH_3$ (22%)
42: R_1 = F; R_2 = $O(CH_2)_8CH_3$ (25%)
43: R_1 = F; R_2 = $O(CH_2)_9CH_3$ (23%)
44: R_1 = F; R_2 = $O(CH_2)_{13}CH_3$ (26%)
45: R_1 = F; R_2 = Br (21%)
46: R_1 = F; R_2 = OMe (23%)
47: R_1 = F; R_2 = NMe_2 (30%)

Scheme 2. General synthesis of pyrazoline derivatives.

NMR results suggests that only the $R(C=S)NH_2$ and $R(C=O)NH_2$ species, more stable, are present. The ^1H NMR spectra of the compounds showed three doublet of doublets in the regions of δ 3.0 and δ 6.0 ppm with $J_{a,b}$ ~ 17.7 Hz, $J_{a,x}$ ~ 4.8 Hz, and $J_{b,x}$ ~ 12.0 Hz, confirming the nonequivalence of hydrogen at Hx (ABX system). NH_2 protons were observed at δ 6.51 ppm (compound 32) or δ 7.92-8.03 ppm (compound **46**) as singlet. In the ^{13}C NMR spectra

signals in the δ 43.0 and δ 59.0 ppm corresponding to C4 and C5 carbons (for details see Supporting Information).

2.2. Spectroscopy techniques

The Raman spectra were recorded in the 50-3500 cm^{-1} region at a resolution of 4 cm^{-1} using a FT-Raman Bruker RFS-100 spectrometer. The Nd:YAG laser line at 1064 nm wavelength has been used as exciting radiation for the Raman measurements. The laser power has been kept at 20 mW, and 1000 or 2000 scans have been averaged for each solid sample. The hydrogen (^{1}H) and carbon (^{13}C) NMR spectra were recorded on Bruker Advance DRX300 (300 MHz) spectrometer. The chemical shifts values (δ) have been reported in parts per million (ppm) with reference to tetramethylsilane (TMS) as internal reference. NMR experiments have been carried out in deuterochloroform ($CDCl_3$) or deuterodimethylsulfoxide (DMSO-d_6). The following abbreviations are used for the multiplicities for proton spectra: s (singlet); d (doublet); dd (double dublet); m (multiplet). Coupling constants (*J*) are reported in Hertz (Hz).

2.3. Computational Methodology

In order to get a full comparison with the spectroscopic data experimentally obtained, full quantum mechanical calculations have been applied to compounds **21**, **29**, **30**, **31**, **32**, **37**, **45** and **46**.

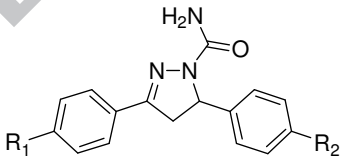

21: R_1 = H; R_2 = $O(CH_2)_8CH_3$
29: R_1 = F; R_2 = Br
30: R_1 = F; R_2 = OMe
31: R_1 = F; R_2 = NMe_2
32: R_1 = F; R_2 = Me

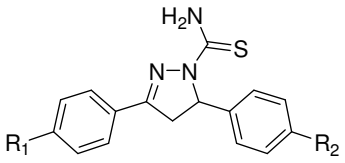

37: R_1 = H; R_2 = $O(CH_2)_8CH_3$
45: R_1 = F; R_2 = Br
46: R_1 = F; R_2 = OMe

Figure 1. Chemical structure of the pyrazolines analogues.

Firstly, the compounds were fully unconstrained optimized to a global minimum point at the potential energy surface using B3LYP functional [30,31] with 6-311G(2d,2p) basis set [32] in the polarizable continuum method IEFPCM [33] as implemented in Gaussian 09 program package [34]. The solvent used was the DMSO since the synthesized compounds are soluble in this solvent. Vibrational harmonic frequencies calculations were performed for each compound in order to obtain the calculated Raman spectra. Those frequencies were scaled by different factors for a better comparison with experimental data. Thermal contributions to Gibbs free energy and other state functions were calculated at 298.15 K and 1 atm. NMR shifts were calculated using the Gauge-Independent Atomic Orbital (GIAO) method [35]. TMS was used as reference and all NMR calculations were performed considering the DMSO dielectric constant.

Then, for a better comparison a scan calculation have been performed in order to obtain the most accurate geometry related to the dihedral which turns the functional group N–CO(NH_2) as it has been done for pyrazinamide ligands [36]. The best (lowest) calculated structure in energetic terms was obtained as displayed in Figure 2 for compound **32**. The optimization of all structures was then based on the general geometry obtained through this scan as depicted in Figure 2.

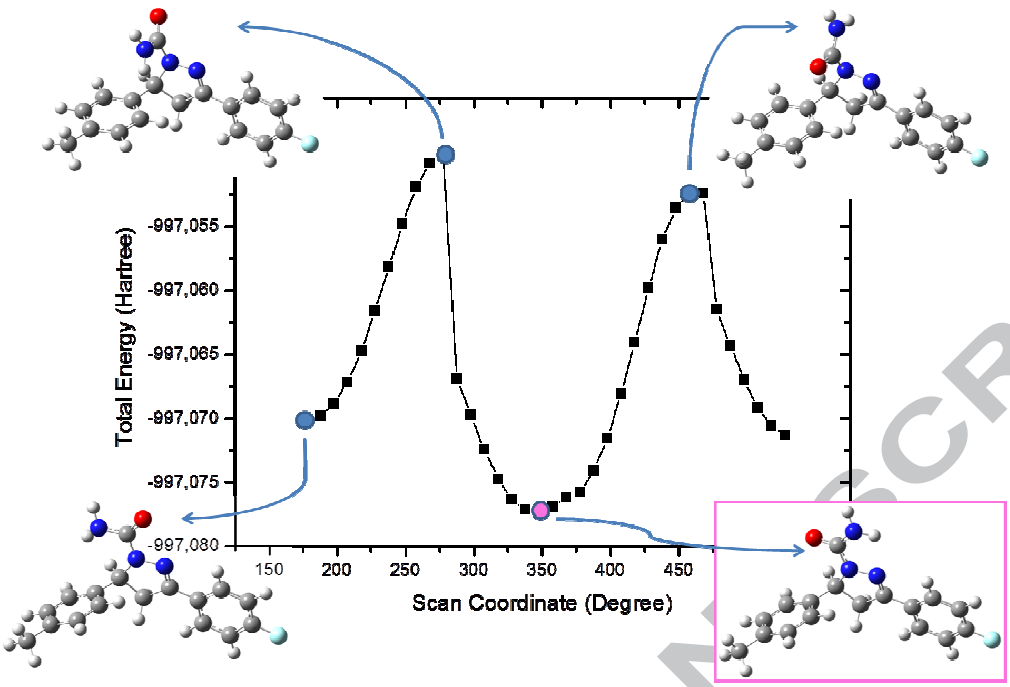

Figure 2. Highlighted at bottom right, the obtained structure in the scan procedure. This structure corresponds to the lowest point in the graphic.

For compounds **21** and **37**, those with a long aliphatic carbon chain, a simulated annealing has been performed in order to achieve a structure with the lowest energy. The method was basically the same used before in Rey's work [37]. Nine geometries in a range of 2 kcal mol^{-1} were chosen in order to perform full DFT calculations using the same level of theory as used for structure optimization. The results point out to the same geometry, in general. All simulated annealing details can be found in the Supplementary Material.

3. RESULTS AND DISCUSSION

Scientists in biosciences field must understand and take into consideration the tautomerism effect and the spatial conformers as a relevant aspect for biological activity. In this sense, the characterization of the pyrazoline derivatives of the representative compounds **32**, and **46** (see scheme 2) is presented in details by NMR, FT-Raman techniques and DFT methods. The results for the compounds **21**, **29**, **31**, **37** and **45** have been subjected to a

similar analysis, and are presented as Supporting Information. The structural characterization of the cited compounds could be regarded as representative of the behavior of the entire series. In the case of the pyrazolines synthesized, a tautomerism effect may occur; namely, the carboxamide/carbothioamide group ($R(C=O)NH_2/R(C=S)NH_2$) may tautomerize to the corresponding (R(C=NH)OH/R(C=NH)SH) species, in the solid state or in solution (see Scheme 3).

3.1. Raman characterization of the tautomeric structures

Raman spectroscopy, due to the sensitivity to the molecular structure and to the well-recognized ability of the Raman effect to detect more than one tautomeric form simultaneously [19], has been chosen to characterize the tautomeric behavior of the synthesized series of pyrazolines derivatives. The pyrazoline derivatives could present a tautomerism as the one presented in Scheme 3.

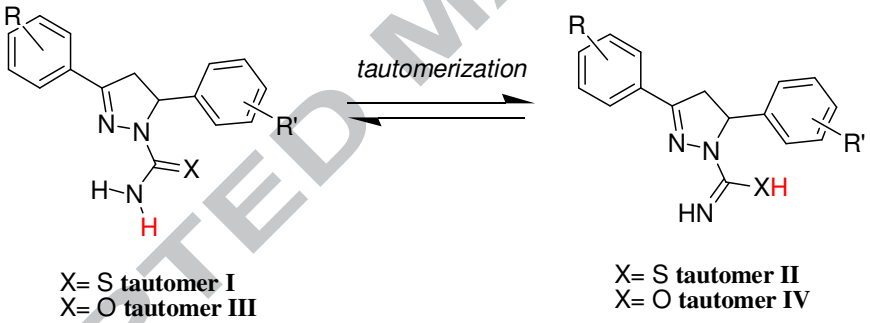

Scheme 3. Tautomeric forms of pyrazoline derivatives.

It should be mentioned that characteristic bands of the tautomers may be found in the Raman spectra: for the carboxamide derivatives, the changes in intensity of the band assigned to C-OH groups compared to C=O would be enough to characterize the presence of different tautomer; similar information would be available from the analysis of the bands assigned to C-SH/C=S in the Raman spectra of the carbothioamides. For the characterization of the tautomeric species, one representative compound of each carboxamide and carbothioamide series are discussed in detail. Figure 3 presents the experimental and DFT calculated Raman

spectrum of compound **46**. An assignment of the Raman spectrum, based on the literature [44] and on theoretical calculations of vibrational wavenumbers, is presented in Table 1.

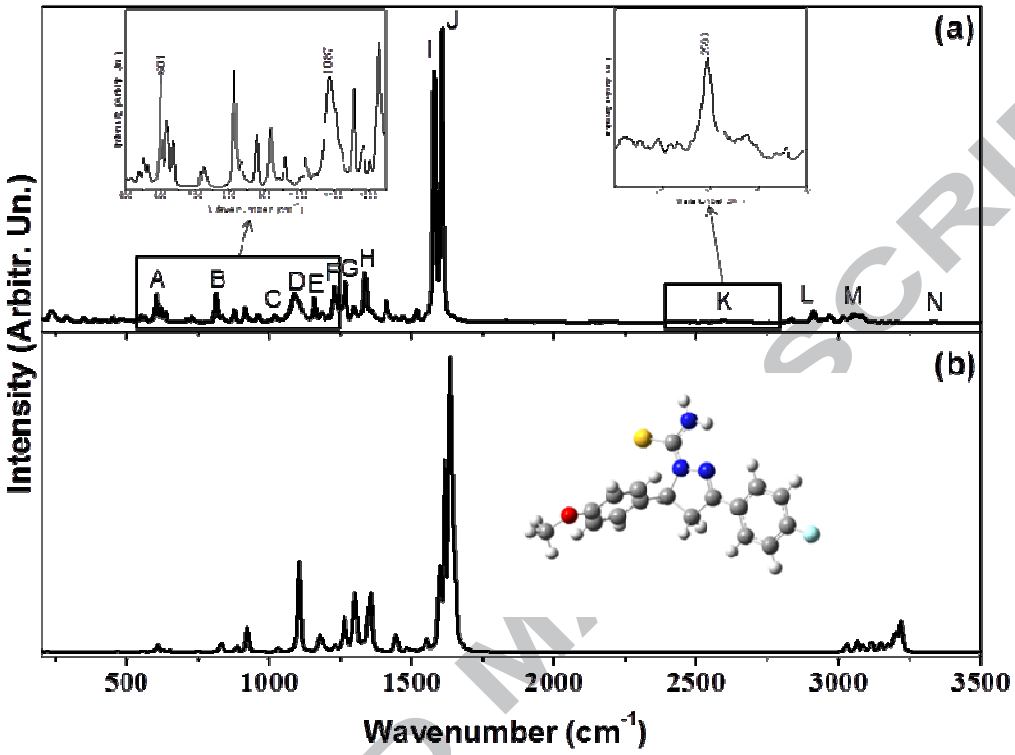

Figure 3. (a) Experimental Raman spectra of the compound **46** in the solid-state; the inset present a zoom in the 500-1250 cm^{-1} and 2400-2700 cm^{-1} regions of the spectrum. (b) Raman-DFT calculated spectrum of compound **46** in DMSO dielectric; the inset represents the DFT-optimized structure for **46**, used for the calculation of the Raman spectrum.

Table 1. Assignment of selected experimental and theoretical Raman band positions for the compound **46** (solid-state).

Reference to Figure 3	*Experimental wavenumber / cm^{-1}*	*Theoretical wavenumber / cm^{-1}*	*Theoretical scaled wavenumber[a] / cm^{-1}*	*Assignment*
A	**601**	605 [b]	599	**νC-S**, **($NCN_{rocking}$)**
B	700-915	731-858	723-867	δ_{oop}C-H
C	1018	1030	1020	ν_{tri}CC aromatic
D	**1094**	1351	1422	**νC=S**
E	1158	1043, 1096	1098, 1154	νCN, νCC
F	1228	1298, 1322	1233, 1256	βCH
G	1266	1368	1300	νCC, νCN, νC-NH_2
H	1334	1489	1414	νCN
I	1577	1614	1582	νCC aromatic + ν_sC=N
J	1604	1614	1582	νCC aromatic + ν_sC=N
K	**2593**	[c]	[c]	**νS-H**
L	2836, 2910, 2965, 2976	3024, 3061, 3083, 3111, 3118, 3145	2873, 2908, 2929, 2955, 2962, 2988	νC-H aliphatic
M	3014, 3036, 3052, 3064, 3078	3168, 3175, 3193, 3199, 3201, 3212, 3214, 3216	3009, 3016, 3033, 3039, 3040, 3051, 3053, 3055	νC-H aromatic
N	3334	3586	3407	$\nu_S NH_2$

[a]Scaled fators: A, B, C = 0.99; D, E, F, G, H = 0.95; I, J = 0.98; L, M, N = 0.95. Most bands are related to conjugated modes, i.e., no simply assignment can be made. [b]The band at 601 cm^{-1} has been found to be assignable to a different mode in the carbothioamide tautomer. [c]The **νS-H** band cannot be identified in this calculation since the structure of compound **46** has been optimized as a thioamide.

The bands assigned in Table 1 are characteristic of the chemical moieties present in compound **46**, but one can observe three bands, two at 601/2593 cm^{-1} assigned to C-SH group and one at 1094 cm^{-1} assigned to the C=S group (bold in Table 1). The presence of the two

groups of bands strongly suggests the presence of both tautomeric forms indicated in Scheme 2. It should be noticed, however, that the relative intensity of the ν(SH) in the Raman spectrum of compound 46 (inset of Figure 3) is considerably lower than what is usually expected for this mode [29]. This unexpected low relative intensity of the band at 2593 cm^{-1} suggests that an additional resonance structure, that presents the C-S group, but deprotonated ($C\text{-}S^-$), may have an important contribution to the structure of the compound **46** in the solid state (see Scheme 4).

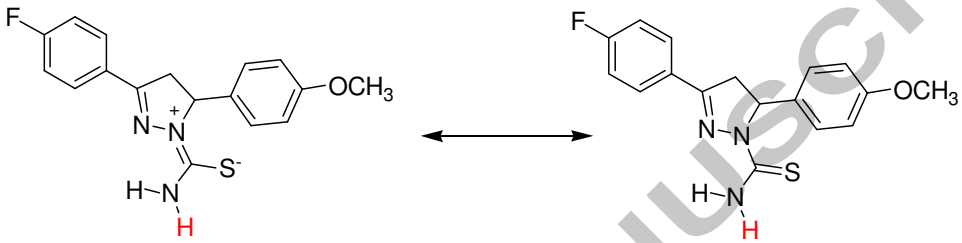

Scheme 4. Resonance structure of the pyrazoline derivatives.

Raman spectra of the carbothioamide compounds **37**, **40**, **45** and **46** have been obtained and a similar analysis can be performed. The intensity ratio between the band assigned to ν(C-S) to the band assigned to ν(C=S), presented in Table 2, changes as a function of the substituent, and one can additionally observe a change when the Raman spectra is acquired for the compounds in chloroform solution.

Table 2. Relative Intensity of the Raman bands νC=S (thioamide tautomer) versus νC-S (thiol tautomer) for carbothioamide compounds in the solid state and in chloroform solution.

Compound	$I_{\nu C=S}/I_{\nu C-S}$	
	Solid-state	**In solution**
(37)	0.88	1.8
(40)	0.87	2.0
(45)	1.52	1.6
(46)	0.98	2.5

One can notice that for the substances in the solid state, compounds **37**, **40** have a similar value of the I(νC=S)/ I(νC–S) intensity ratio, and for compound **46** there is an increase in the contribution of the thioamide tautomer, which increases even further for compound **45.** This change may be related with electron withdrawing properties of the substituents; compounds **37** and **40** present moderately donating O-atom connected directly to the aromatic rings, but compound **46** presents a moderately withdrawing and one moderately donating group, while compound **45** presents two moderately withdrawing substituents. These statements are summarized in Scheme 5. For the compounds in solution the I(νC=S)/ I(νC–S) relative intensity has changed in the direction of the carboxithioamide tautomer (see Table 3), indicating that interactions with solvent plays an important role in the tautomeric equilibrium of this family of compounds.

for electron-donating substituents

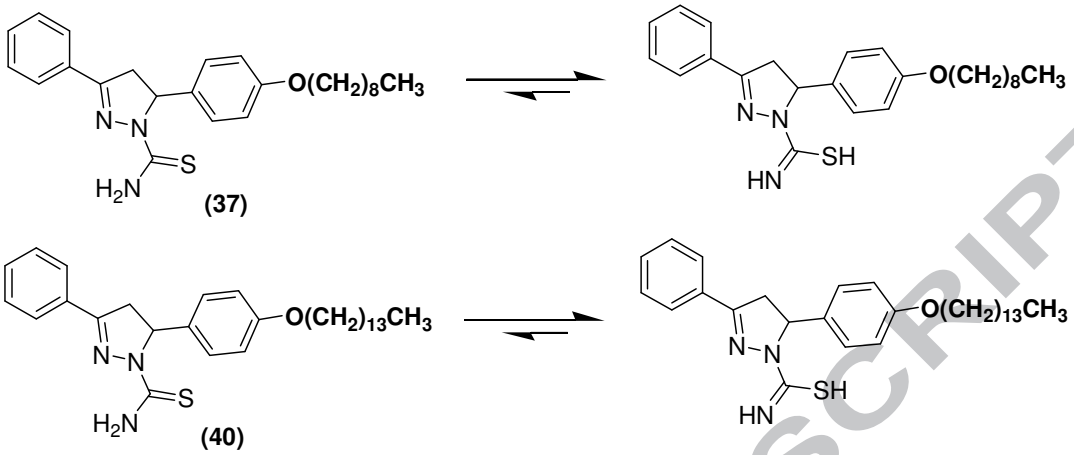

for two electron-withdrawing substituents

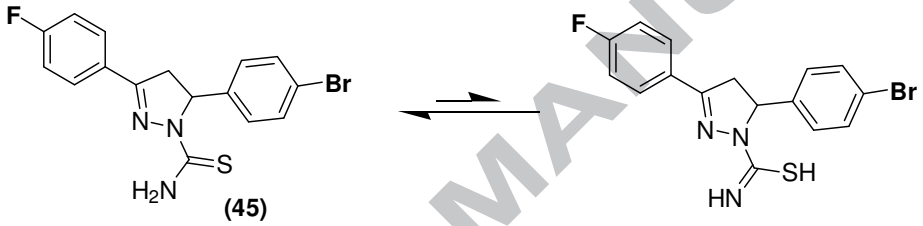

for electron-donating and electron-withdrawing substituents

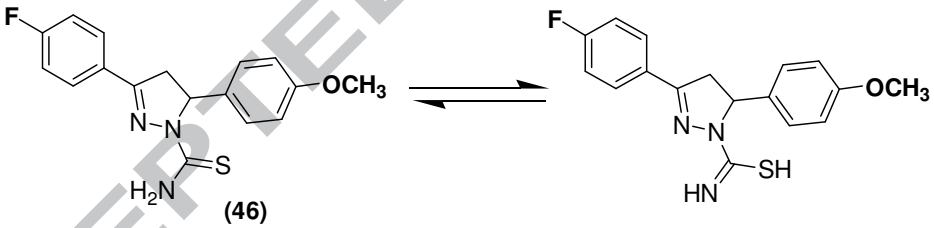

Scheme 5. Tautomerization of the thioamide to the thiol form.

For the carboxamides a case study is presented in Figure 4, which presents the experimental Raman spectrum of compound **32** in the solid state, along with the DFT-calculated spectrum in DMSO solution (the optimized DFT structure is presented as inset); the vibrational assignment for the Raman spectrum is presented in Table 3. The Raman spectrum in Figure 4(a) presents reasonable resolution and high signal-to-noise ratio, and one can notice from the assignment in Table 3 a medium-weak intensity band assigned to νC=O; however, it is not straightforward to assign specific bands to the C-OH group present in tautomer II (Scheme 3) of this series of compounds, because the bands assignable to C-O and C-N groups are assigned to quite similar regions of the Raman spectrum. One can notice, on

the other hand, that the bands assigned to C-N groups, present both in carboxamide and carbothioamide compounds, are more intense in the carboxamide compounds (comparing, for example Figure 1 and 3); although not conclusive, the change in intensity may be an indication of the presence of the tautomer II for this series of compounds. In Figure 4(b), the DFT calculated Raman spectrum can be seen for the compound **32** and shows an impressive correspondence with the experimental one.

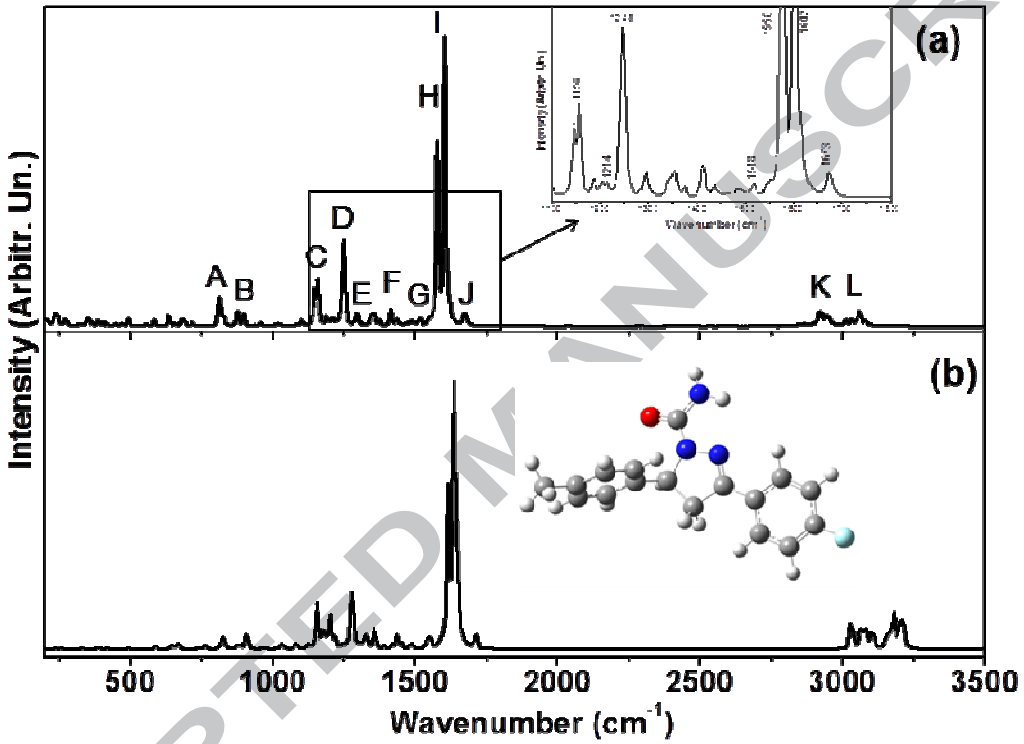

Figure 4. (a) Experimental Raman spectra of the compound **32** in the solid-state; the inset presents a zoom in to the 1100 to 1800 cm^{-1} spectral range. (b) Raman-DFT calculated spectrum of compound **32** in DMSO dielectric; the inset represents DFT-optimized structure for **32**, used for the calculation of the Raman spectrum.

Table 3. Assignment of selected experimental (solid-state) and theoretical Raman band positions for the compound **32**.

Reference to Figure 4	*Experimental wavenumber / cm^{-1}*	*Theoretical wavenumber / cm^{-1}*	*Theoretical scaled wavenumber[a] / cm^{-1}*	*Assignment*

A	683; 717; 812; 877	734; 741; 744; 831; 857	727; 734; 737; 823; 848	$\delta C-H_{arom}$
B	897	907	898	$\nu_{tri}(CC)$
C	1158	1156	1144	νCN, νCC
D	1248	1454	1250	νCN
E	**1295**	**1357**	**1276**	**νCN, νCC, νC-OH**[b]
F	1354; 1376; 1412	1436; 1448; 1454	1350; 1361; 1367	$\beta C-H_{arom}$
G	**1518**	**1613; 1616**	**1516; 1519**	**νC=N**
H	**1576**	1636; 1648; 1652	**1538; 1549; 1553**	**νC=N + νCC_{arom}**
I	1608			νCC_{arom}
J	**1673**	**1712**	**1678**	**νC=O**
K	2922; 2941; 2951	3031; 3063; 3076; 3079; 3099; 3108	2879; 3910; 2922; 2925; 2944; 2953	$\nu C-H_{aliph}$
L	3012; 3034; 3059	3159; 3175; 3178; 3196; 3199; 3210; 3212	3001; 3017; 3019; 3036; 3039; 3050; 3051	$\nu C-H_{arom}$

[a]Scaled fators: A, B, C = 0.99; D = 0.86; E, F, G, H, I = 0.94; J = 0.98; K, L = 0.95. Most bands like the one in 1454 cm^{-1} (non-scaled theoretical value) are related to conjugated modes, i.e., no simply assignment can be made. [b]The νC-OH band cannot be identified in this calculation since the structure of compound **32** has been optimized as a ketone, for clarifying.

3.2. Computational studies on the tautomeric structures

In order to check on the stability of the series of pyrazoline derivatives, and also to get as much spectroscopic information as it could be provided by the unconstrained optimizations, NMR calculations were performed in addition to the Raman spectrum. All structures were characterized as a minimum in the potential energy surface.

The Raman spectra obtained for compounds **32** and **46** were of remarkable agreement in comparison with the experimental ones as already discussed (see Figure 3(b) for compound **46** and Figure 4(b) for compound **32**). This noteworthy agreement between experiment and

calculation enabled the assignment of the Raman spectra with a great contribution from the calculated spectra, as one can notice in Tables 1 and 3, which showed the most important bands with the respective assignments.

The main bands of the calculated Raman spectrum of compound **46** are in good agreement with the experimental one. Some scaled factors were applied in order to improve this agreement for all bands, even for those bands that it would not be necessary, in order to comply a statistical meaning. Since the highest the scaled factor, better the description of the band wavenumber, it can be seen that only the theoretical value found for the band labeled as "D" in Tables 2 is far from the experimental data. This specific spectral region is quite convoluted to be assigned by the DFT calculations, once different conjugated modes have been found in this region. The very same statement could be done for the Raman spectroscopic data found for compound **32**, if one looks closely to Table 3. Once again the calculated bands are in a good agreement to the band positions form the experimental spectrum. The assignments of some normal vibrational modes might be very difficult to determine since in most theoretical calculations many vibrational modes are conjugated with others and the displacement vectors imply in different attribution when comparing with experimental data; this has not been observed in the data obtained for the pyrazoline derivatives presented in this work. Therefore, the data show in Tables 1 and 3 are in fact good for this level of calculations.

In order to identify the tautomeric equilibrium, the NMR-GIAO calculations have been performed for compound **32** and **46**. From these calculations the differences between the protonated and non-protonated structures can be stablished. Such results are showed in Figure 5. The results found for the ^{1}H-NMR shifting seems to provide a good linear fit between experimental and DFT calculations, and so the calculation results could be used for deciding which tautomeric structure is present.

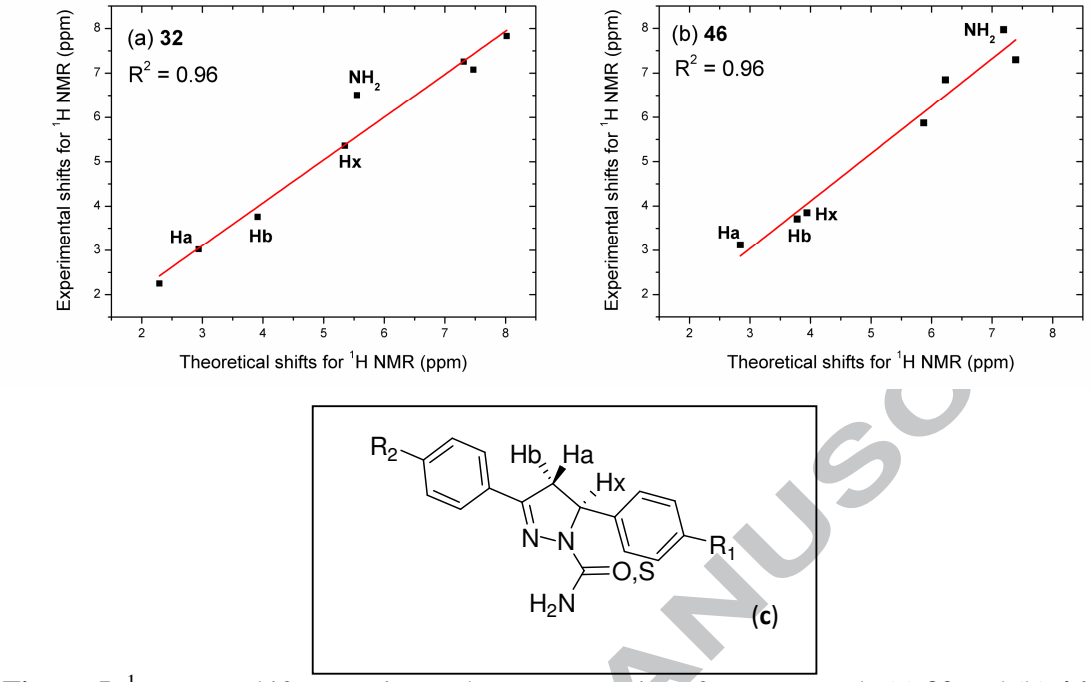

Figure 5. ^{1}H-NMR shifts experimental-DFT comparison for compounds (a) **32** and (b) **46**. (c) Labelled scheme for hydrogens Ha, Hb, Hx and NH_2 to better correlate the data in plots (a) and (b).

As can be seen in Figure 5, the theoretical results for ^{1}H-NMR calculated under the DMSO dielectric constant are in very good agreement with the experimental ones. The R^2 data from fitting linear regression is equal to 0.96 for both comparisons in Figures 5(**a**) and 5(**b**). The largest disagreement regards to the NH_2 hydrogen atoms for both compounds **32** and **46**, which is in fact interesting due to the mixture of tautomers that exists in real solution. The other hydrogen signals are in almost perfect accordance to those found in solution. Here, is interesting to highlight the signals of hydrogens Ha, Hb and Hx, according to the labels presented in Figure 5(**c**). For compound 32, the NMR experimental signals found were 3.02 (dd, 1H, Ha, $J_{a,x}$= 5.1 Hz, $J_{a,b}$= 18.0 Hz); 3.76 (dd, 1H, Hb, $J_{b,x}$= 12.0 Hz, $J_{b,a}$= 18.0 Hz); 5.36 (dd, 1H, Hx, $J_{x,a}$= 5.1 Hz, $J_{x,b}$= 12.0 Hz); 6.51 (sl, 2H, N-H). For compound 46, the NMR experimental data are 3.12 (dd, 1H, Ha, $J_{a,x}$= 3.0 Hz, $J_{a,b}$= 18.0 Hz); 3.71 (s, 3H, CH_3); 3.85 (dd, 1H, Hb, $J_{b,x}$= 12.0 Hz, $J_{b,a}$= 18.0 Hz); 5.87 (dd, 1H, Hx, $J_{x,a}$= 3.0 Hz, $J_{x,b}$= 12.0 Hz); 7.92-8.03 (m, 4H, Ar e N-H). All other NMR data can be found at the Supporting Information.

Another important factor correlated to the differences between these two tautomers is the thermodynamics. Through the frequencies calculations the ΔG values between the protonated and non-protonated species suggests that the $R(C=S)NH_2$ and $R(C=O)NH_2$ species are more stable than the R(C=NH)SH and R(C=NH)OH species. The calculated difference between compounds **46** and its protonated counterpart is 21.34 kcal mol^{-1}, while for compound **32** and its tautomer one can find a difference of 22.50 kcal mol^{-1}. Both values are in the same order and point out to the original compounds **32** and **46** as the most stable in this comparison. From such Gibbs energies results is possible to suggest that both species can be found in solution but probably there would be a large amount of **32** and **46** than the protonated ones. This calculation results for the pyrazoline compounds in solution agrees with the observed for the Raman of the carbothioamide compounds in solution (Table 1), in which it has been verified that tautomer I structures presented larger Raman intensity than those for tautomer II.

4. CONCLUSIONS

In this work the synthesis of a series of thirty new pyrazolines has been successfully performed, and the compounds have been characterized by ^{1}H and ^{13}C NMR. In order to understand in more details the tautomeric behavior in the solid and solution states, a joint experimental-computational study using density functional theory, FT-Raman and NMR investigation were carried on the tautomerism of pyrazole-carbothioamide and pyrazole-carboxamide compounds.

The Raman spectra of selected compounds were conclusive for the carbothioamide compounds and indicated that the tautomeric distribution changes significantly from solid to solution, as tautomer I seems to be more stable in solution than in the solid state. Density functional theory calculations have played an important role in this analysis, and presented a good accordance that allowed a vibrational assignment of the Raman spectra. Such analysis might assist the experimentalists to further discuss some assignments. Also, a very good agreement was achieved by the NMR calculations in DMSO solution. The results indicates that in fact in a real solution the tautomers must be present since only the NH_2 hydrogen shift have a large disagreement between experiment and calculation. Furthermore, the calculated

thermodynamics indicates the stability of the compounds in the tautomer I form, in agreement with the Raman spectroscopy indicated for the carbothioamide compounds.

ACKNOWLEDGMENTS

The authors gratefully acknowledge UFJF, CAPES, CNPq and FAPEMIG for fellowships. GFSA thanks CNPq for a research fellowship. SA thanks FAPEMIG for a fellowship. This work is a collaboration research project of members of the Rede Mineira de Química (RQ-MG) supported by FAPEMIG.

ASSOCIATED CONTENT

Supporting Information. Experimental procedures and spectroscopic data for the compounds, computational data and experimental Raman data and assignment on selected compounds are available.

REFERENCES

[1] V. Monga, K. Goyal, M. Steindel, M. Malhotra, D.P. Rajani, S.D. Rajani, Med. Chem. Res. 23 (2014) 2019–2032;

[2] F.E. Hawaiz, M.K. Samad, J. Chem. 3 (2012) 1613-1622;

[3] K.A. Parmar, J.R. Vihol, Y.M. Dabhi, S.D. Sutariya, J. Chem. Pharm. Res. 4 (2012) 1584-1588;

[4] O.A. Miqdad, N.M. Abunada, H.M. Hassaneen, A.S.M.A. Samaha, Int. J. Chem. 3 (2011) 20-31;

[5] V. Gressler, S. Moura, A.F.C. Flores, D.C. Flores, P. Colepicolo, E. Pinto, J. Braz. Chem. Soc. 21 (2010) 1477-1483;

[6] M.A. Ali, M. Shaharyar, Bioorg. Med. Chem. 15 (2007) 1896-1902;

[7] M. Shaharyar, A.A. Siddiqui, Bioorg. Med. Chem. Lett. 16 (2006) 3947-3949;

[8] S. Bano, K. Javed, S. Ahmad, I.G. Rathish, S. Singh, M.S. Alam, Eur. J. Med. Chem. 46 (2011) 5763-5768;

[9] K.M. Amin, S.M. Abou-Seri, F.M. Awadallah, A.A.M. Eissa, G.S. Hassan, M.M. Abdulla, Eur. J. Med. Chem. 90 (2015) 221-231;

[10] J.P. Jasinski, J.A. Golen, S. Samshuddin, B. Narayana, H.S. Yathirajan, Crystals 2 (2012) 1108-1115;

[11] H.A. Soleiman, A.K. Khalafallah, H. Abd-Ellatif, Eur. J. Chem. 3 (2012) 316-321;

[12] P.D. Lokhand, B.Y. Waghamare, S.S. Sakate, Ind. J. Chem. 44b (2005) 2338-2342;

[13] M.N.A. Nasr, S.A. Said, Arch. Pharm. Pharm. Med. Chem. 336 (2003) 551-559;

[14] H.I. Boshoff, D.J. Wilson, J. Neres, N.P. Labello, R.V. Somu, C.G. Xing, C.E. Barry, C.C. Aldrich, J. Med. Chem. 51 (2008) 7495-7507;

[15] M. Komoda, H. Kakuta, H. Takahashi, Y. Fujimoto, S. Kadoya, F. Kato, Y. Hashimoto, Bioorg. Med. Chem. 9 (2001) 121-131;

[16] M.A. Palafox, V.K. Rastogi, S. Kumar, H. Joe, Spectrochim. Acta A 111 (2013) 104-122;

[17] B.J.A.N. Almeida, L. Lapinski, R. Fausto, J. Mol. Struct. 1025 (2012) 74-83;

[18] H. Rostkowska, L. Lapinski, I. Reva, B.J.A.N. Almeida, M.J. Nowak, R. Fausto, J. Phys. Chem. A 115 (2011) 12142-12149;

[19] D.R.C. Matazo, R.A. Ando, A.C. Borin, P.S. Santos, J. Phys. Chem. A 112 (2008) 4437-4443;

[20] J.A. Vila, Y.A. Arnautova, Y. Vorobjev, H.A. Scheraga, Proceedings of the National Academy of Sciences of the United States of America 108 (2011) 5602-5607;

[21] T. Barclay, M. Ginic-Markovic, M.R. Johnston, P. Cooper, N. Petrovsky, Carbohydr. Res. 347 (2012) 136-141;

[22] A.A. Kaczor, T. Wrobel, Z. Karczmarzyk, W. Wysocki, E. Mendyk, A. Poso, D. Matosiuk, M. Pitucha, J. Mol. Struct. 1051 (2013) 188–196;

[23] R.M. Claramunt, M.A García, C. López, S. Trofimenko, G.P.A. Yap, I. Alkorta, J. Elguero, Magn. Reson. Chem. 43 (2005) 89–91;

[24] M. Franco-Pérez, R. Moya-Hernández, A. Rojas-Hernández, A. Gutiérrez, R. Gómez-Balderas, J. Phys. Chem. B 115 (2011) 13593-13598;

[25] E. Tasal, M. Kumalar, Spectrochim. Acta A 101 (2013) 204–217;

[26] E. Tasal, M. Kumalar, Spectrochim. Acta A 95 (2012) 282–299;

[27] E. Tasal, M. Kumalar, Spectrochim. Acta A 96 (2012) 548–562;

[28] E. Tasal, M. Kumalar, Spectrochim. Acta A 124 (2014) 687–696;

[29] M.H. Youssoufi, P.K. Sahu, D.D. Agarwal, M. Ahmad, M. Messali, S. Lahsasni, T.B. Hadda, Med. Chem. Res. (2014) DOI 10.1007/S00044-014-1297-1;

[30] A.D. Becke, J. Chem. Phys. 98 (1993) 5648-5652;

[31] C. Lee, W. Yang, R.G. Parr, Phys. Rev. B. 37 (1988) 785-789;

[32] K. Raghavachari, J.S. Binkley, R. Seeger, J.A. Pople, J. Chem. Phys. 72 (1980) 650-654;

[33] G. Scalmani, M.J. Frisch, J. Chem. Phys. 132 (2010) 110-115;

[34] M.J. Frisch, G.W. Trucks, H.B. Schlegel, G.E. Scuseria, M.A. Robb, J.R. Cheeseman, G. Scalmani, V. Barone, B. Mennucci, G.A. Petersson, H. Nakatsuji, M. Caricato, X. Li, H.P. Hratchian, A.F. Izmaylov, J. Bloino, G. Zheng, J.L. Sonnenberg, M. Hada, M. Ehara, K. Toyota, R. Fukuda, J. Hasegawa, M. Ishida, T. Nakajima, Y. Honda, O. Kitao, H. Nakai, T. Vreven, J.A. Montgomery, Jr., J.E. Peralta, F. Ogliaro, M. Bearpark, J.J. Heyd, E. Brothers, K.N. Kudin, V.N. Staroverov, R. Kobayashi, J. Normand, K. Raghavachari, A. Rendell, J.C. Burant, S.S. Iyengar, J. Tomasi, M. Cossi, N. Rega, M.J. Millam, M. Klene, J.E. Knox, J.B. Cross, V. Bakken, C. Adamo, J. Jaramillo, R. Gomperts, R.E. Stratmann, O. Yazyev, A.J. Austin, R. Cammi, C. Pomelli, J.W. Ochterski, R.L. Martin, K. Morokuma, V.G. Zakrzewski, G.A. Voth, P. Salvador, J.J. Dannenberg, S. Dapprich, A.D. Daniels, Ö. Farkas, J.B. Foresman, J.V. Ortiz, J. Cioslowski, D.J. Fos, GAUSSIAN 09, Revision A.02, GAUSSIAN, Inc.: Wallingford CT, 2009;

[35] J.R. Cheeseman, G.W. Trucks, T.A. Keith, M.J. Frisch, J. Chem. Phys. 104 (1996) 5497-5509;

[36] P.A.S. Oliveira, L.M. Sartori, N.A. Rey, H.F. Dos Santos, M.A.L. De Oliveira, L.A.S. Costa, J. Braz. Chem. Soc. 24 (2013) 1732-1738;

[37] L.V. De Freitas, C.C.P. Da Silva, J. Ellena, L.A.S. Costa, N.A. Rey, Spectrochim. Acta A 116 (2013) 41-48;

[38] X. Su, H. Xu, Q. Guo, G. Shi, J. Yang, Y. Song, X. Liu, J. Polym. Sci., Part A: Polym. Chem. 46 (2008) 4529–4541;

[39] J. Hasegawa, M. Hamada, T. Miyamoto, K. Nishide, T. Kajimoto, J. Uenishi, M. Node, Carbohydr. Res. 340 (2005) 2360-2368;

[40] A. Hasan, A. Abbas, M.N. Akhtar, Molecules 16 (2011) 7789-7802;

[41] X. Zhang, J. Kang, P. Niu, J. Wu, W. Yu, J. Chang, J. Org. Chem. (2014) dx.doi.org/10.1021/jo501844x |;

[42] T.A.A. Yahyaa, J.H. Abdullaha, M.A.H. Al-Ghorafi, S.H. Yassin, J. Chem. Pharm. Res. 6 (2014) 234-238;

[43] P. Pujari, Ramesh V., M. Chandran, D. Paul, A.R. Bhat, K. Krishnakumar, World J Pharm Res. 3 (2014) 1268-1276;

[44] D.W. Mayo, F.A. Miller, R.W. Hannah, Course Notes on the Interpretation of Infrared and Raman Spectra, John Wiley & Sons, Hoboken – USA, 2003.

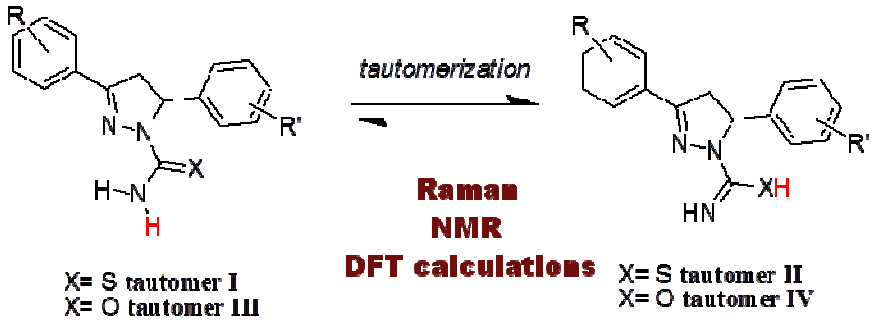

X= S tautomer I
X= O tautomer III

X= S tautomer II
X= O tautomer IV

- Synthesis of a series of new pirazolines derived from chalcones is described
- NMR and Raman spectroscopy study on the tautomerization equilibrium in the series of compounds
- Energy and vibrational computational DFT calculations allowed understanding the tautomerization equilibrium.